Frequency Tracking Method and Compensation Parameters Optimization to Improve Capacitor Deviation Tolerance of the Wireless Power Transfer System

Wang, Yi ; Yang, Zhongping ; Lin, Fei; Dong, Jianning; Bauer, Pavol

DOI
10.1109/TIE.2022.3232657

Publication date
2023

Document Version
Final published version

Published in
IEEE Transactions on Industrial Electronics

Citation (APA)
Wang, Y., Yang, Z., Lin, F., Dong, J., & Bauer, P. (2023). Frequency Tracking Method and Compensation Parameters Optimization to Improve Capacitor Deviation Tolerance of the Wireless Power Transfer System. *IEEE Transactions on Industrial Electronics*, *70*(12), 12244-12253. https://doi.org/10.1109/TIE.2022.3232657

Frequency Tracking Method and Compensation Parameters Optimization to Improve Capacitor Deviation Tolerance of the Wireless Power Transfer System

Yi Wang, *Graduate Student Member, IEEE*, Zhongping Yang, *Member, IEEE*, Fei Lin, *Member, IEEE*, Jianning Dong, *Member, IEEE*, and Pavol Bauer, *Senior Member, IEEE*

***Abstract*—Compensation capacitors are naturally susceptible to manufacturing defects and aging effects, leading to the degraded performance of a wireless power transfer (WPT) system. This article focuses on the compensation parameters optimization during the design stage and control strategy during the operation phase to improve the inherent capacitor error tolerance of the WPT system. The Sobol sensitivity method is applied to rank the importance of deviations of three capacitors on the transfer characteristics, and then the method of tracking the secondary resonance frequency is proposed. The numerical method is applied to find the optimal compensation parameters, with the constraint that the output voltage change caused by the shift of the designed compensation condition is limited to be less than $\pm$5%. Experimental results show that with the proposed frequency tracking method and compensation parameter optimization, the deviation tolerance index is decreased from 0.485 to 0.363, showing an improvement of 25.2%, and the minimum power factor is increased from 0.78 to 0.89. Besides, the characteristics of constant primary coil current and voltage gain are almost not affected.**

***Index Terms*—Compensation errors, detuning tolerance, frequency tracking, parameter optimization, wireless power transfer (WPT).**

Nomenclature

U_{P}	Output voltage of the primary inverter.
U_{S} (U_{S0})	Real (ideal) input voltage of the secondary rectifier.
L_{P} (L_{S})	Self-inductance of the primary (secondary) coil.
L_{r}	Primary series compensation inductance.
C_{r} (C_{r0})	Real (ideal) primary parallel compensation capacitance.
C_{P} (C_{P0})	Real (ideal) primary series compensation capacitance.
C_{S} (C_{S0})	Real (ideal) secondary series compensation capacitance.
M	Mutual inductance.
R_{E}	Equivalent load resistance.
ω (ω_0)	Real (ideal) resonance frequency.
k_{Us}	Ratio of the output voltage with capacitor errors to that of the ideal compensation condition.
Q_{in}	Primary inverter quality factor.
Q_{O}	Load quality factor.
L_{PR}	Ratio of the primary coil's self-inductance to the primary series compensation inductance.
k_{r}, k_{P}, k_{S}, k_{ω}	Ratios of C_{r}, C_{P}, C_{S}, and ω to C_{r0}, C_{P0}, C_{S0}, and ω_0, respectively.
λ	Power factor.
χ	Defined index representing the performance variations of the WPT system.
$U_{\mathrm{C_r}}$, $U_{\mathrm{C_P}}$, $U_{\mathrm{C_S}}$	Voltages of three compensation capacitors.
$k_{\mathrm{UC_r}}$, $k_{\mathrm{UC_P}}$, $k_{\mathrm{UC_S}}$	Ratios of three compensation capacitors' voltages with capacitance deviations to their ideal values, respectively.

Manuscript received 19 July 2022; revised 15 November 2022; accepted 14 December 2022. Date of publication 4 January 2023; date of current version 9 June 2023. This work was supported by the China Scholarship Council. *(Corresponding author: Fei Lin.)*

Yi Wang, Zhongping Yang, and Fei Lin are with the School of Electrical Engineering, Beijing Jiaotong University, Beijing 100044, China (e-mail: 16121534@bjtu.edu.cn; zhpyang@bjtu.edu.cn; flin@bjtu.edu.cn).

Jianning Dong and Pavol Bauer are with the DCE&S/EEMCS, Delft University of Technology, 2624 CP Delft, The Netherlands (e-mail: j.dong-4@tudelft.nl; p.bauer@tudelft.nl).

Color versions of one or more figures in this article are available at https://doi.org/10.1109/TIE.2022.3232657.

Digital Object Identifier 10.1109/TIE.2022.3232657

η	Transfer efficiency from the primary inverter output to the secondary rectifier input.
$\Delta\eta$	Change in the transfer efficiency caused by capacitor errors.
ψ	Defined index representing the capacitor error tolerance of the WPT system.
$k_{\mathrm{U_S-max}}$, $k_{\mathrm{U_S-min}}$	Maximum and minimum values of $k_{\mathrm{U_S}}$.
$k_{\mathrm{UC_r-max}}$, $k_{\mathrm{UC_P-max}}$, $k_{\mathrm{UC_S-max}}$	Maximum values of $k_{\mathrm{UC_r}}$, $k_{\mathrm{UC_P}}$, $k_{\mathrm{UC_S}}$, respectively.
$\Delta\eta_{\max}$	Maximum drop in the transfer efficiency.
k_{M} (k_{R})	Ratio of the actual mutual inductance (load resistance) to the rated one.
$k_{\mathrm{U_S-MR}}$ ($k_{\mathrm{I_P-MR}}$)	Ratio of the output voltage (current of the primary coil) caused by variations in mutual inductance and load resistance after tracking frequency to the rated value.
η_{S}	Transfer efficiency from the primary three-phase input to the secondary rectifier output.
$\Delta\eta_{\mathrm{S\text{-}max}}$	Maximum drop in η_{S}.
$k_{\mathrm{r\text{-}d}}$, $k_{\mathrm{P\text{-}d}}$, $k_{\mathrm{S\text{-}d}}$	Designed k_{r}, k_{P}, and k_{S} during the manufacturing stage.

I. Introduction

WIRELESS power transfer (WPT) technology can avoid the problems of wear and contact sparks caused by the traditional plug-in type. Besides, WPT systems can still work in severe weather conditions such as rain and snow, as there are no exposed wires [1], [2]. Therefore, WPT technology has received wide attention and research in the fields of AGVs [3], underwater machines [4], electric vehicles [5], [6], and so on.

The main function of the resonant network is to reduce the reactive power and improve the transfer efficiency of WPT systems. However, the requirements for resonance are very stringent. Once resonance parameters deviate from their ideal values, the reactive power of a WPT system will increase and its transfer efficiency may decrease. Due to the inevitable accuracy issues and discrete capacitances of commercial capacitors, precise compensation is time-consuming and labor-intensive in the manufacturing phase. Not only does it undoubtedly increase the cost of a WPT system, but it is also elusive for mass production. Besides, changes in the ambience, such as the temperature, and aging will also lead to changes in capacitances at the operation stage, which is essentially determined by the properties of the dielectric, the capacitor construction, and the manufacturing parameters [7], [8], [9], [10]. As a result, nonideal compensation is a common problem for WPT systems. Measures need to be taken to improve the detuning tolerance of WPT systems to lower the impacts of device parameter drifts on the system performance.

Putting the WPT system into a nonresonant state deliberately could help to obtain an improved characteristic. Through the design of detuning compensation parameters proposed in [11], the SS compensated system has a relatively stable output power when the coupling coefficient changes within a large range. Zhang et al. [12], [13] found that when the WPT system works at a certain detuning compensation point, the SS network obtains a characteristic of constant voltage output. Although the WPT system working in a detuned state reduces the stringent requirements for resonance parameters to a certain extent, the above research still requires the system to work at a specific detuning point. When the actual system deviates from the designed condition, the desired characteristics may not be maintained.

Real-time control is necessary to maintain the desired performance considering there may be variations in load, coupling, and others [5]. The frequency tracking method is widely used to adjust the output power [14], maintain zero-voltage-switching (ZVS) [15], [16], and optimize the transfer efficiency [17]. However, these studies do not analyze the impacts of capacitance deviations on the system transfer characteristics and control targets. When the compensation capacitances deviate from the rated values, the expected control goals may not be realized, especially when the frequency splitting is taken into consideration. Controllable capacitors proposed in [18] and [19] could realize ideal compensation and eliminate compensation errors theoretically. However, a controllable capacitor consists of one or two high-frequency switches connected in reverse series and a capacitor in parallel. These extra switches will introduce conduction loss into the WPT system and depress its transfer efficiency. In addition, the control complexity and device expense would rise and the system reliability would be weakened, if each compensation position is occupied by a controllable capacitor. Therefore, a simple and effective method with little impact on the original transfer characteristics is urgently needed to enhance the capacitance deviation tolerance of the WPT system.

In the previous work, we have analyzed the influence of capacitor errors on the output voltage, power factor, transfer efficiency and capacitors' voltage stresses of the *LCC-S* compensated WPT system, and have proposed a general coupler design method [20]. The *LCC-S* topology is applied due to its constant primary coil current and voltage gain characteristics [21], [22]. Besides, the *LCC* circuit extends the freedom of system design since its voltage gain is only determined by the ratio of the mutual inductance to the primary series compensation inductance under ideal compensation conditions [23], [24]. The error tolerance of a 22-kW WPT system designed with the proposed method is improved compared with the conventional design process. However, when the errors of three compensation capacitors are $\pm 10\%$, the transfer characteristics still change significantly. The output voltage will be reduced by 21.5% at most, while the minimum power factor is only 0.78. Besides, the voltages of capacitors may also have a nonnegligible increase. So, further measures are needed to improve the error tolerance of WPT systems.

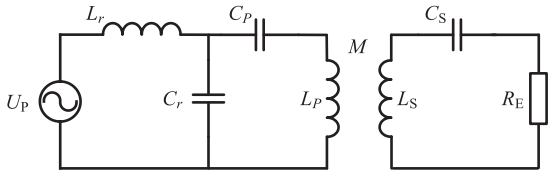

Fig. 1. Typical schematic diagram of *LCC-S* compensation topology.

To further improve the capacitance deviation tolerance of the WPT system, this article first uses the Sobol sensitivity analysis method to compare the importance of three compensation capacitors to the error tolerance of the *LCC-S* compensated WPT system, and find the most influential one. Then, the compensation error of that compensation position can be eliminated through the real-time monitoring of the capacitance and frequency tracking, so that the error tolerance can be improved. Since ideal compensation has relatively high requirements for the components, the compensation circuit is adjusted to an imperfect state during the design phase to further reduce the impacts of capacitance deviations on the transfer characteristics. The deviations of three capacitors are considered simultaneously because capacitance deviations are unavoidable and unpredictable. The numerical analysis and parameter sweeping method are applied to optimize compensation parameters.

This article is organized as follows. In Section II, the Sobol sensitivity analysis method is applied to rank the importance of three compensation capacitors on the transfer characteristics of the *LCC-S* compensated WPT system. The expressions of the output voltage and power factor with the frequency tracking strategy are derived. Section III proves the effectiveness of the proposed frequency tracking strategy and compensation parameter optimization theoretically. Besides, the impacts of the proposed frequency tracking method and compensation parameter optimization on the characteristics of constant primary coil current and voltage gain of the *LCC-S* topology are analyzed. Verification experiments are carried out in Section IV, while Section V concludes this article.

II. Sensitivity Analysis of Capacitor Error Tolerance and Frequency Tracking Strategy

A. Capacitor Error Tolerance Analysis

The schematic of the *LCC-S* circuit is shown in Fig. 1. When compensation parameters satisfy the following:

$$\omega_0 L_r = \frac{1}{\omega_0 C_r} = \omega_0 L_P - \frac{1}{\omega_0 C_P}, \omega_0 L_S = \frac{1}{\omega_0 C_S}. \quad (1)$$

The output voltage can be expressed as

$$U_{S-0} = \frac{M}{L_r} U_P. \quad (2)$$

Generally, inductors do not suffer from aging and temperature effects. Compared to inductances, capacitances are less immune to factors such as manufacturing tolerance, aging, ambient temperature, humidity, etc. So, only capacitor errors are discussed in this article. Although losses in the inverter, compensation inductor, and capacitors (generally calculated with the dissipation factor listed in the datasheet), coupler, and rectifier will also affect the performance of a WPT system and they may vary with temperature, their impacts are limited, especially for a high-efficiency system. As a result, circuit and component losses are ignored in the theoretical analysis below, except for the efficiency calculation.

The impacts of capacitor errors on the transfer characteristics of WPT systems have been analyzed in [20]. The expressions of the output voltage, power factor, transfer efficiency, and voltage stresses of compensation capacitors of a detuned WPT system are derived, among which the change ratio of the output voltage k_{U_S} is shown as follows:

$$k_{U_S} = \frac{U_S}{U_{S-0}} = \frac{1}{\left|(1+jaQ_O)\left[(1-k_r)\left(\frac{Q_{in}}{j-aQ_O}+b\right)+1\right]\right|} \quad (3)$$

where

$$a = 1 - \frac{1}{k_S}, b = L_{PR}\left(1-\frac{1}{k_P}\right) + \frac{1}{k_P} \quad (4)$$

$$Q_{in} = \frac{\omega_0 M^2}{L_r R_E}, Q_O = \frac{\omega_0 L_S}{R_E}, \ L_{PR} = \frac{L_P}{L_r} \quad (5)$$

$$C_r = k_r C_{r-0}, \ C_P = k_P C_{P-0}, \ C_S = k_S C_{S-0} \quad (6)$$

the load impedance of the inverter is written by

$$Z_{in} = j\omega L_r + \frac{j\omega L_r}{-k_r + \frac{1}{\frac{Q_{in}}{j-aQ_O}+b}}. \quad (7)$$

The power factor can be calculated by

$$\lambda = \frac{\mathrm{Re}[Z_{in}]}{|Z_{in}|} \quad (8)$$

where Re[] serves as the real part of the value in brackets.

The extremes of the output voltage and other abovementioned indices are used to evaluate the impacts of capacitor errors on WPT systems. Then, the design constraints are obtained to meet the system requirements on the transfer characteristics considering $\pm 10\%$ capacitor errors (i.e., $0.9 \le k_r, k_P, k_S \le 1.1$). $\pm 10\%$ is a typical value determined in this article after taking into account the accuracy of available commercial capacitors, system cost, and influence on the system. With the proposed simplified and easy-to-follow system design process in [20], a 22-kW WPT system with improved capacitor error tolerance for an electric bus is designed. The parameters of the designed system are shown in Table I. The analysis below is based on this designed coupler, but the methodology is applicable to other coupling coils.

B. Sensitivity Analysis

Although the capacitor error tolerance of the WPT system is improved by designing the coupler, the performance deprecation is not negligible when there are deviations in the capacitances. Hence, further measures to improve the error tolerance are desired. In the previous analysis, the importance of the errors of three capacitors is not distinguished. Since three compensation

TABLE I
SYSTEM SPECIFICATION

Variables	Parameters
Input voltage	510 V
Output voltage	510 V
Rated power	22 kW
Working frequency (kHz)	85
Specifications of the primary coil	4 turns, 800 mm
Specifications of the secondary coil	6 turns, 700 mm
Primary coil inductance L_P (μH)	61.3
Secondary coil inductance L_S (μH)	100.1
Mutual inductance M (μH)	20.7

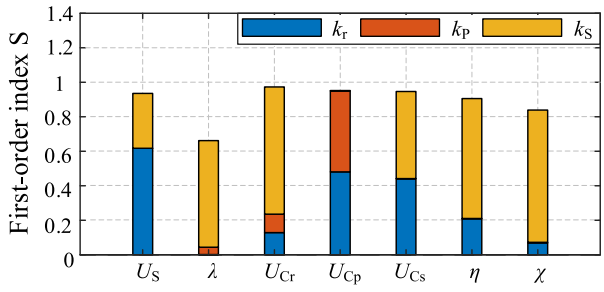

Fig. 2. Results of the Sobol sensitivity analysis.

capacitors resonate with different inductors at different positions according to (1), for example, C_r resonates with L_r while C_S resonates with L_S, they may affect the performance of WPT systems to varying degrees. Given the unpredictability and inevitability of the errors of three compensation capacitors, it may be feasible to strike a tradeoff between the error tolerance and the ease and economy of the implementation of improvement measures by reducing the capacitor error of the most influential compensation position. So next, the importance of the errors of three compensation capacitors will be sorted first.

Sensitivity analysis is an effective way to investigate the influence of numerous parameters in a system. The Sobol method based on variance decomposition is a universal global sensitivity analysis method not limited to the function expression. Here, the first-order index is used to represent the importance value. Given a model with the form $Y = f(X_1, X_2, \ldots X_k)$, the first-order sensitivity coefficient of the ith factor X_i is written as [25], [26]

$$S_i = \frac{V\left[E\left(Y|X_i\right)\right]}{V\left(Y\right)} \tag{9}$$

where $E(Y|X_i)$ means that the mean of Y is taken over all possible values of X but X_i, $V[E(Y|X_i)]$ is the variance of the argument $E(Y|X_i)$ with all possible values of X_i taken over. $V(Y)$ is the total variance of the output.

In this article, χ is defined as follows to evaluate the performance variations caused by capacitance deviations:

$$\begin{aligned}\chi = {} & \alpha_1 \cdot (|k_{U_S} - 1| + 1 - \lambda) \\ & + \alpha_2 \cdot (|k_{UC_r} - 1| + |k_{UC_P} - 1| + |k_{UC_S} - 1|) \\ & + \alpha_3 \cdot |\Delta\eta|\end{aligned} \tag{10}$$

where α_1, α_2, and α_3 are the weight coefficients, and their values are 0.5, 0.1, and 1, respectively, in this article. χ is calculated from the variations of the output voltage, power factor, capacitors' voltages, and transfer efficiency caused by capacitance deviations. The larger the χ, the more severely the WPT system is affected by the capacitor errors. Since k_{US}, k_{UCr}, k_{UCp}, and k_{UCs} are all 1 with an ideally compensated system, the performance variations are expressed as the results of subtracting 1 from these voltage-related indicators. For the power factor λ, its variation is expressed as "1-λ" as λ will never exceed 1. It should be mentioned that the weight coefficients can be changed from case to case, but the analysis method in this article is universal.

With the optimized coupler in [20] and ±10% capacitor errors considered, the calculation steps of the Sobol analysis are summarized below [27].

1) Specify the number of variables d and sampling ranges. In this article, $d = 3$, and sampling ranges for (k_r, k_P, k_S) are all from 0.9 to 1.1.
2) Generate an $N \times 2d$ sample matrix from the Sobol sequence. N is the number of sampling points and is 30000 in this article to ensure accuracy.
3) Construct the calculation matrix according to the sampling matrix and calculate U_S, λ, U_{Cr}, U_{Cp}, U_{Cs}, η, and χ separately at each point.
4) Calculate the variance of the model output and the sensitivity indices using the Monte Carlo estimator.

Then, the importance indices of the errors of three compensation capacitors are obtained, as shown in Fig. 2.

According to Fig. 2, the error of the secondary compensation capacitor, k_S, is the most influential factor while k_P only affects U_{Cp} significantly. Although k_r affects U_S, U_{Cp}, and U_{Cs}, it has little effect on the overall capacitor error tolerance.

C. Frequency Tracking Method Analysis

Since k_S mainly affects the error tolerance of the WPT system, the capacitor error tolerance can be improved by reducing or even eliminating the error of the secondary series capacitor. To strengthen the inherent tolerance of the WPT system against capacitance deviations, this article focuses on the compensation parameter optimization during the design stage and control strategy during the operation stage. According to (1), the compensation error of the secondary capacitor can be eliminated by tracking the operating frequency as the secondary resonance frequency theoretically, that is, the operating frequency is adjusted from ω_0 to ω. ω can be calculated by

$$\omega L_S = \frac{1}{\omega k_S C_{S-0}}. \tag{11}$$

Then the relationship between k_ω and k_S could be written as

$$k_S = \frac{1}{k_\omega^2}. \tag{12}$$

During the system operation stage, the real capacitance of the secondary capacitor can be obtained by measuring its voltage and current in real time. Then the secondary resonance frequency could be calculated with the measured secondary capacitance

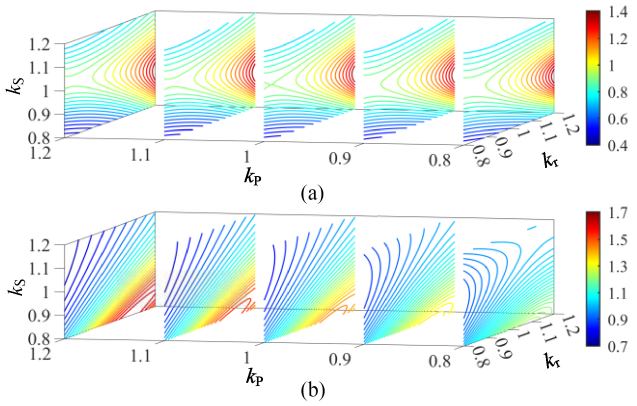

Fig. 3. Variations of the output voltage change ratio with capacitor errors when the freqency tracking method is applied or not. (a) Without frequency tracking. (b) With frequency tracking.

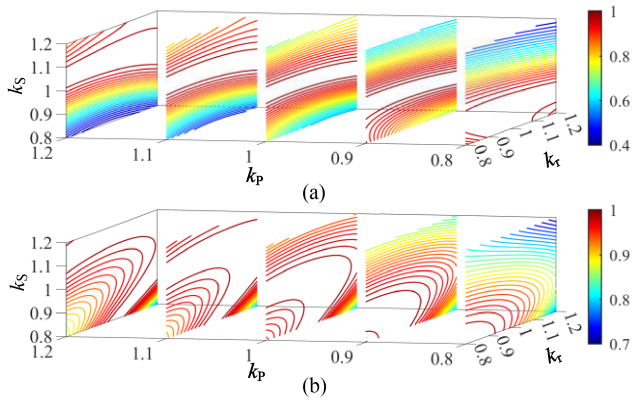

Fig. 4. Variations of the power factor with capacitor errors when the frequency tracking method is applied or not. (a) Without frequency tracking. (b) With frequency tracking.

and the known secondary inductance. The value could be transferred to the primary through Wi-Fi, Bluetooth, or other means, and then the primary controller adjusts the operating frequency to realize frequency tracking. From the point of view of improving capacitance deviation tolerance only, there may be an optimal frequency. However, the actual capacitances of all three capacitors need to be known to calculate the minimum χ, which will undoubtedly increase the cost and complexity of the system hardware. So, the method of tracking the secondary resonance frequency is applied here.

Although the compensation error of the secondary can be eliminated by the frequency tracking method, the relative compensation errors of the primary may increase. For example, the impedance of the primary parallel compensation capacitance C_{r} is $\omega_0 C_{\mathrm{r0}}$ with ideal compensation, while it is $\omega_0 k_{\mathrm{r}} C_{\mathrm{r0}}$ with capacitance deviations. When the proposed frequency tracking method is applied, the impedance becomes $k_\omega \omega_0 k_{\mathrm{r}} C_{\mathrm{r0}}$. So, the variations of transfer characteristics of WPT systems due to capacitor errors and frequency tracking strategy will be analyzed next. With capacitor errors and the frequency tracking strategy, the output voltage change ratio and the load impedance of the inverter are rederived, as shown as follows:

$$k_{U_S} = \frac{U_S}{U_{S-0}} = \frac{1}{\left|\left(1-k_\omega^2 k_r\right)\left(-jk_\omega Q_{in}+b'\right)+1\right|} \tag{13}$$

$$Z_{in} = j\omega_0 k_\omega L_r + \frac{j\omega_0 k_\omega L_r}{-k_\omega^2 k_r + \frac{1}{-jk_\omega Q_{in}+b'}} \tag{14}$$

where

$$b' = L_{PR}\left(1-\frac{1}{k_\omega^2 k_P}\right)+\frac{1}{k_\omega^2 k_P}. \tag{15}$$

The power factor could be calculated with Z_{in}. Figs. 3 and 4 compare the variations of the output voltage and power factor with capacitor errors when the proposed frequency tracking strategy is applied or not.

According to Figs. 3 and 4, the characteristics of the output voltage and power factor are significantly altered by the varied impedance matching state caused by the frequency tracking strategy. First, the application of the frequency tracking strategy significantly affects the extreme values of the output voltage and power factor caused by capacitor errors. When (k_{r}, k_{P}, k_{S}) vary between 0.8 to 1.2, the output voltage change ratio varies from 0.4 to 1.4 with the fixed operating frequency, while the varying range becomes from 0.7 to 1.7 when the proposed frequency tracking method is applied. For the primary inverter, it could output less reactive power with the frequency tracking method as the minimum power factor is increased from 0.4 to 0.7.

On the other hand, the frequency tracking strategy also affects the changing trend of the output voltage and power factor with capacitor errors. Each section has 25 contour lines in Figs. 3 and 4. The larger the distance between adjacent contour lines, the less sensitive the system transfer performance is to capacitance variations in that region. From their changing trend and colors, it can be found that adjusting compensation parameters can also improve the error tolerance of WPT systems. Adjusting compensation parameters here means designing ($k_{\mathrm{r\text{-}d}}$, $k_{\mathrm{P\text{-}d}}$, $k_{\mathrm{S\text{-}d}}$). With the inevitable $\pm 10\%$ capacitor errors taken into consideration, (k_{r}, k_{P}, k_{S}) in the actual operation could be any values within $\pm 10\%$ of ($k_{\mathrm{r\text{-}d}}$, $k_{\mathrm{P\text{-}d}}$, $k_{\mathrm{S\text{-}d}}$) centered. When $k_{\mathrm{r\text{-}d}}$ is 0.9, the actual k_{r} may vary arbitrarily between 0.8 and 1, while its variation range is from 0.9 to 1.1 when $k_{\mathrm{r\text{-}d}}$ is 1 for the ideal compensation. There are some parameter ranges that make the system transfer performance insensitive to capacitance changes. For example, as shown in Fig. 3(b), the output voltage is not sensitive to capacitor errors if the primary parallel capacitor is designed to be under-compensated and the primary and secondary series capacitors are in an over-compensated state during the design stage, that is, $k_{\mathrm{r}} < 1$, $k_{\mathrm{P}} > 1$ and $k_{\mathrm{S}} > 1$, while the output voltage can be relatively stable as long as $k_{\mathrm{P}} > 1$ and $k_{\mathrm{S}} < 1$ are avoided after the frequency tracking method applied.

The same method can be used to analyze the variations in the transfer efficiency and voltage stresses of the capacitors, which are not shown here due to the limited length. To strike a tradeoff between the output voltage, power factor, and other indicators, it is necessary to quantitatively evaluate the impacts of capacitance deviations on the overall system performance to optimize compensation parameters, which will be carried out

TABLE II
CALCULATION RESULTS OF THE PROPOSED FREQUENCY TRACKING AND COMPENSATION PARAMETERS OPTIMIZATION

NO.	$k_{r\text{-}d}$	$k_{P\text{-}d}$	$k_{S\text{-}d}$	k_{U_S}		λ	k_{UC_r}	k_{UC_P}	k_{UC_S}	$\eta(\%)$	ψ
				k_{U_S-max}	k_{U_S-min}	λ_{min}	k_{UC_r-max}	k_{UC_P-max}	k_{UC_S-max}	$\Delta\eta_{max}(\%)$	
1	1	1	1	1		1	1	1	1	95.46	0.432
				1.136	0.721	0.758	1.496	1.270	1.182	-0.836	
2	0.965	1.080	1.035	0.950		0.999	0.925	0.896	0.918	95.41	0.391
				1.152	0.781	0.806	1.579	1.246	1.229	-0.599	
3	1.040	1.065	1.100	0.950		0.999	0.896	0.981	0.906	95.42	0.361
				1.263	0.859	0.905	1.524	1.355	1.339	-0.353	

in the next section. The frequency tracking strategy obviously improves the stability of the power factor since the $\lambda_{\min}$ is increased from 0.4 to 0.7, but it is difficult to intuitively judge the impact of the frequency tracking strategy on the output stability. Therefore, the effectiveness and advantages of implementing a frequency tracking strategy need to be quantitatively assessed, which will also be done next.

III. COMPENSATION PARAMETERS OPTIMIZATION TOGETHER WITH FREQUENCY TRACKING AND THEIR IMPACTS

A. Compensation Parameters Optimization

The previous theoretical analysis shows that it is feasible to adjust the compensation parameters during the manufacturing phase to improve the capacitor error tolerance of WPT systems, together with the proposed frequency tracking method during the operation stage. The optimization of compensation parameters becomes the key issue to be solved next. Since compensation parameters have different impacts on the output voltage, power factor, and other transfer characteristics indicators, compromise among these characteristics is inevitable. Therefore, a comprehensive index reflecting the capacitor error tolerance of the WPT system ψ is defined as follows:

$$\begin{aligned}\psi = {} & \beta_1 \cdot (k_{U_S-\max} - k_{U_S-\min} + 1 - \lambda_{\min}) \\ & + \beta_2 \cdot (k_{UC_r-\max} + k_{UC_P-\max} + k_{UC_S-\max} - 3) \\ & + \beta_3 \cdot |\Delta\eta_{\max}| \end{aligned} \tag{16}$$

where β_1, β_2, and β_3 are the weight coefficients, and their values are 0.5, 0.1, and 1, respectively, in this article. To evaluate the effectiveness of the compensation parameter optimization, the extreme values of the output voltage and other indices caused by the $\pm 10\%$ capacitance deviations are applied in (16), which is different from (10).

To find the optimal compensation parameters, the parameter sweeping method is applied here. ($k_{r\text{-}d}$, $k_{P\text{-}d}$, $k_{S\text{-}d}$) are swept from 0.9 to 1.1 with intervals of 0.005, respectively. For each group of ($k_{r\text{-}d}$, $k_{P\text{-}d}$, $k_{S\text{-}d}$), the extremes in (16) and ψ are calculated, and the optimal result is shown in Table II (NO. 3), compared with the results of conditions when the compensation parameters are not adjusted and the frequency tracking method is not used (NO. 1), and when only the compensation parameters are optimized (NO. 2). To avoid great changes in the transfer characteristics of the WPT system, the change ratio of the output voltage at the designed compensation parameters to the ideal compensation is limited to be less than $\pm 5\%$.

It should be mentioned that the results of NO. 2 and NO. 3 at the designed points are calculated relative to those of NO. 1, while $k_{U_S\text{-max}}$, $k_{U_S\text{-min}}$, $k_{UCr\text{-max}}$, $k_{UC_P\text{-max}}$, and $k_{UC_S\text{-max}}$ are relative to their corresponding conditions. For example, the output voltage of NO. 3 when ($k_{r\text{-}d}$, $k_{P\text{-}d}$, $k_{S\text{-}d}$) are (1.040, 1.065, 1.100) is decreased to 0.950 times the rated value M/L_r, while the maximum output voltage caused by capacitance deviations is $1.12 \cdot M/L_r$, thus $k_{U_S\text{-max}}$ is 1.263.

With compensation parameters optimized alone, the extremes of the output voltage would not change much compared with the ideal compensation condition. However, when the frequency is tracked, $k_{US\text{-max}}$ is increased from 1.125 to 1.263, and $k_{US\text{-min}}$ is increased too, from 0.781 to 0.859. The most significant change happens in the power factor, $\lambda_{\min}$ is increased to 0.905, while it is just 0.758 without any improvement measure and 0.806 with compensation parameter optimization only. Theoretically, the capacity of the primary inverter could be reduced by 20.21% and 15.16% compared with NO. 1 and NO. 2, respectively. The transfer efficiency becomes more stable after the compensation parameters optimized and frequency tracked. Although the cost is that $k_{UCr\text{-max}}$, $k_{UCP\text{-max}}$, and $k_{UCS\text{-max}}$ rise, these absolute values of the maximum voltages of three capacitors do not change significantly as k_{UCr}, k_{UCP}, and k_{UCS} are smaller than 1. On the whole, the capacitance deviation tolerance is improved from 0.432 (without optimization) and 0.391 (with compensation parameters optimized only) to 0.361 with the proposed compensation parameter optimization and frequency tracking strategy.

B. Impacts of the Frequency Tracking Method

Since the designed compensation parameters in this article deviate from the ideal values shown in (1), the aforementioned excellent constant primary coil current and voltage gain features of the *LCC-S* network may be destroyed. Therefore, the variations of the primary coil current and voltage gain with the load and mutual inductance are analyzed here. The change ratio of the primary coil current I_P and output voltage caused by the proposed frequency tracking method and compensation parameter optimization can be derived as follows:

$$k_{I_P-MR} = \frac{I_P}{I_{P-0}} = \frac{1}{k_\omega \left| (1-k_\omega^2 k_r)\left(-jk_\omega \frac{k_M^2 Q_{in}}{k_R} + b'\right) + 1 \right|} \tag{17}$$

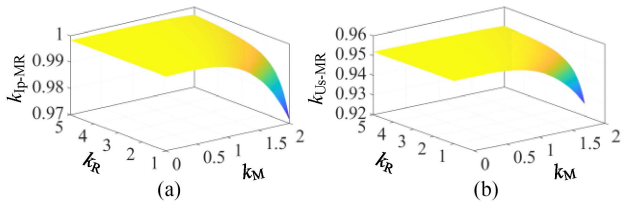

Fig. 5. Variations of the change ratios of the primary coil current and the output voltage with the load resistance and mutual inductance. (a) Variations of the change ratio of the primary coil current. (b) Variations of the output voltage change ratio.

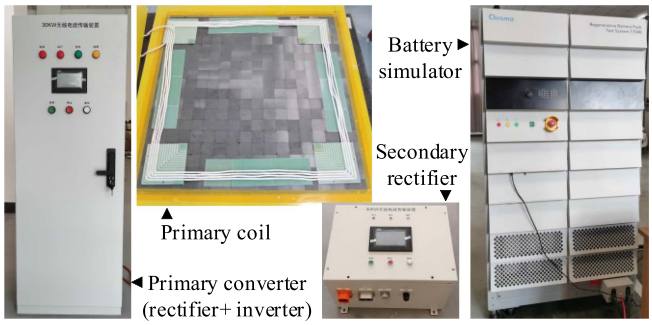

Fig. 6. Experimental platform.

$$k_{U_S-MR} = \frac{U_S}{U_{S-0}} = \frac{1}{\left|(1-k_\omega^2 k_r)\left(-jk_\omega \frac{k_M^2 Q_{in}}{k_R} + b'\right)+1\right|}. \tag{18}$$

The variations of k_{I_P-MR} and k_{U_S-MR} with k_{M} and k_{R} are plotted in Fig. 5 when k_{M} is limited from 0 to 2 and k_{R} varies from 1 to 5.

When the mutual inductance is greater than the rated value and the load resistance is near the rated one, the primary coil current will decrease with the decrease of the load resistance and the increase of the mutual inductance. As for the voltage gain, its value will be smaller than *Lr*/*M*, and its amplitude reduction trend is similar to that of the primary coil current. However, k_{I_P-MR} and k_{U_S-MR} decrease by no more than 3% compared to the designed condition even when the mutual inductance is doubled and the load resistance is maintained at the rated value. It should be noted that that condition will not occur in the acutal operation and is used for theoretical analysis only, as its output power will be almost four times the rated value. Therefore, the constant primary coil current and voltage gain characteristics remains almost unchanged with the proposed frequency tracking method and compenation parameters optimization.

IV. Verification Experiments

A. Experimental Platform

To verify the effectiveness of the proposed frequency tracking strategy and compensation parameter optimization, experiments were carried out on the 22-kW WPT prototype, as shown in Fig. 6. The coupler designed by [20] was used and the parameters of the experimental setup are shown in Table I. Same as the experimental setup in [20], the input source was a three-phase programmable ac power supply, and a Chroma 17040 battery simulator operated in constant resistant (CR) mode was used as the load to ensure the consistency of the input and load among different experiments.

Tektronix voltage probe THDP0100 and current probe TCP0150 were used to measure the voltages and currents of the circuit. The voltage stresses of compensation capacitors were calculated from the capacitances and measured currents. The data sampled by the oscilloscope were outputted to calculate the power factor. Since it is challenging to obtain the ac–ac efficiency accurately, the system transfer efficiency η_{S} from the three-phase input to the secondary rectifier output was measured by the PA3000 power analyzer.

Polypropylene film capacitors of the DTR series manufactured by Shenzhen Dawn Electronic Co. Ltd. were used as compensation capacitors. The capacitances were measured by the Microtest 6630 LCR meter. Since the capacitors were finite and the capacitances were discontinuous, actual capacitances in experiments were slightly different from their expected values. For instance, the theoretical capacitances of the ideal compensation condition (C_{r}, C_{P}, C_{S}) were (172.04 nF, 87.18 nF, 34.65 nF), while the actual capacitances were (171.96 nF, 87.11 nF, 34.67 nF). However, the errors between the actual and expected values were very small and could be neglected.

B. Error Tolerance Verification

Three series of verification experiments were conducted, corresponding to three groups in Table II, respectively. The conditions in which extreme values of the transfer characteristics indicators occurred (i.e., the output voltage, power factor, transfer efficiency, and voltage stresses of the compensation capacitors) were carried out separately. Some waveforms are shown in Fig. 7 and the experimental results are listed in Table III.

It could be seen from Fig. 7(b) and (d) that when the system worked in the minimum power factor conditions, the load impedance of the primary inverter was capacitive regardless of whether the compensation parameters were optimized or not. This was not conducive to the efficient transfer of energy. However, the situation changed when the frequency tracking method was used along with the compensation parameter optimization. According to the theoretical calculation, the minimum power factor and the minimum transfer efficiency occurred simultaneously for NO. 3. The inductive impedance, as shown in Fig. 7(f), made the primary inverter work in a ZVS state, which was favorable for efficiency characteristics.

According to Tables II and III, there were some errors between the experimental results and theoretical analysis. This was partly because the impacts of parasitic parameters were ignored in the theoretical calculation, such as the losses of converters, parasitic resistances of the coils and compensation capacitors, etc. On the other hand, the deviations between the actual compensation capacitances and the expected values were also the cause of the experimental errors. However, the experimental errors of the output voltage and power factor were less than 5% and the errors of voltage stresses of compensation capacitors were smaller than

TABLE III
EXPERIMENTAL RESULTS

NO.	$k_{r\text{-}d}$	$k_{P\text{-}d}$	$k_{S\text{-}d}$	U_S (V)		λ	U_{C_r} (V)	U_{C_P} (V)	U_{C_S} (V)	η_s(%)	ψ
				k_{U_S-max}	k_{U_S-min}	λ_{min}	k_{UC_r-max}	k_{UC_P-max}	k_{UC_S-max}	$\Delta\eta_{s-max}$(%)	
1	1.000	0.999	1.000	495.4		0.99	700.7	890.5	2460.0	93.2	0.485
				1.124	0.684	0.78	1.483	1.277	1.200	-5.9	
2	0.968	1.082	1.033	459.8		0.98	708.5	795.3	2321.0	95.0	0.383
				1.174	0.800	0.86	1.426	1.272	1.313	-2.5	
3	1.040	1.062	1.104	463.8		0.98	628.3	875.8	2374.1	94.8	0.363
				1.264	0.860	0.89	1.473	1.252	1.274	-0.6	

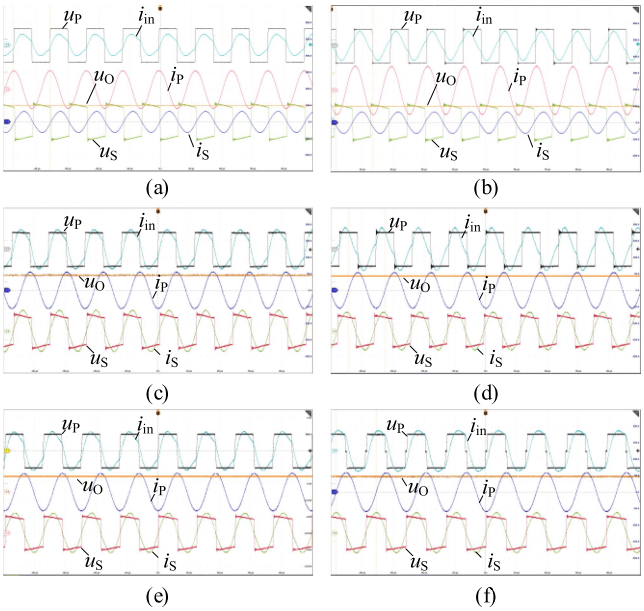

Fig. 7. Experimental platforms of voltages and currents. i_{in} is the output current of the primary inverter while u_{O} is the secondary rectified output voltage. Voltages: 500 V/div. Currents: 100 A/div for (a) and (b), and 50 A/div for others. Time: 10 μs/div. Without optimization, (a) ideal compensation condition and (b) the minimum power factor condition. Compensation parameters optimized only, (c) ideal compensation condition and (d) the minimum power factor condition. The frequency tracking strategy applied and compensation parameters optimized simultaneously. (e) Ideal compensation condition and (f) the minimum power factor condition.

10%. In the theoretical calculation, the quality factors of the coils were set to 200, which were conservation values and might be lower than the actual values, resulting in a high measured transfer efficiency from the three-phase input to the secondary rectified output.

With the frequency tracking strategy and compensation parameters optimization applied, the output voltage of the designed compensation condition was reduced from 495.4 to 463.8 V, with a drop rate of 6.4%, which was almost the same as that of the compensation parameters adjusted only condition. When the $\pm$10% capacitor errors were considered, the minimum output voltage was increased from 338.9 V to 398.8 V, showing an increased rate of 17.6%, while it was increased by 11.6% with compensation parameters optimized only. Besides, the minimum power factor was increased from 0.78 to 0.86 after the compensation parameters were optimized. When the frequency tracking method was also implemented, the minimum power factor could be further increased to 0.89. As a result, the apparent power of the inverter output can be reduced by up to 12.4%, which is beneficial to reducing the capacity of the inverter and the system cost. Although the indices of capacitor voltages were not improved much, the transfer efficiency was increased from 93.2% to 94.8% at the designed compensation condition, which was a considerable achievement with an air gap of 20 cm. The reason for the increase in efficiency lied in that the primary inverter worked in the ZVS state after adjusting compensation parameters. Another reason was that the losses on the capacitors were reduced due to the decrease in the voltages of the capacitors. When the frequency tracking strategy was conducted, the transfer efficiency was slightly lower than that of compensation parameters optimized only condition at the designed point (NO. 2), which was about 0.2% less and could be ignored. Another benefit was that the maximum drop in the transfer efficiency was reduced greatly from 5.9% to 0.6%, which was because the ZVS region was widened. However, the transfer efficiency would be reduced by up to 2.5% when compensation parameters were optimized only. Although the maximum voltage rising rate increased from 12.4% to 26.4%, the overall capacitor error tolerance was improved from 0.485 to 0.363, showing an improvement rate of 25.2%, while that of the compensation parameters optimized condition was only 21.0%. So, the experimental results proved that the proposed frequency tracking method and compensation parameters optimization could effectively improve the capacitance deviation tolerance of the WPT system.

C. Impacts on the Characteristics of the Constant Primary Coil Current and Voltage Gain

To explore the impacts of the proposed frequency tracking strategy and compensation parameter optimization on the characteristics of the constant primary coil current and voltage gain, experiments with the mutual inductance and load changed were performed. The changes in the mutual inductance were realized by adjusting the air gap between the primary coil and the secondary coil. Experiment results were shown in Fig. 8. "∞" of k_{R} means the secondary was open. When the air gap was adjusted from 16 to 32 cm, the mutual inductance was reduced from 26.6 to 11.5 μH.

According to Fig. 8(a), the primary coil current increased with k_{R} and the air gap. When the air gap was 16 cm, the condition with $k_{\text{R}} = 1$ was not conducted as its output power would exceed the rated value. The biggest rise in the primary coil current happened when k_{R} was increased from 1 to ∞, 41.1 to 43.5 A,

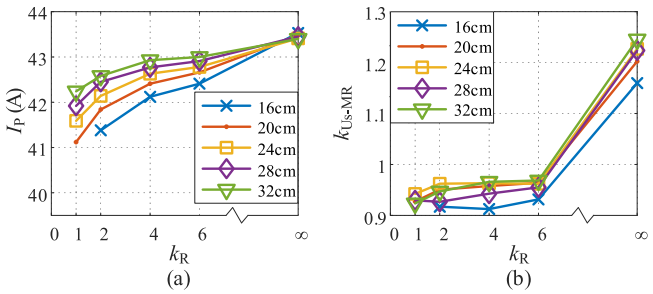

Fig. 8. Variations of I_P and $k_{US\text{-}MR}$ with the air gap and k_R. (a) I_P. (b) $k_{US\text{-}MR}$.

with an increasing rate of 5.8%. It can be found from Fig. 8(b) that when the air gap was changed between 16 to 32 cm and k_R was increased from 1 to 6, $k_{US\text{-}MR}$ was varied from 0.91 to 0.97. The most obvious change in $k_{US\text{-}MR}$ occurred when the WPT system changed from the loaded state to open, with $k_{US\text{-}MR}$ around 1.2. This was caused by the transfer characteristics of the capacitor-filtered rectifier whose output voltage would increase with the increase of the load resistance. So, the constant primary coil current and voltage gain characteristics of the *LCC-S* compensation network were not affected by the proposed frequency tracking strategy and compensation parameter optimization.

V. Conclusion

In this article, the frequency tracking strategy and compensation parameter optimization were proposed and implemented to improve the capacitor error tolerance of the WPT system. The Sobol sensitivity method was used to rank the importance of errors of three capacitors on the transfer characteristics of the WPT system (i.e., the output voltage, power factor, transfer efficiency, and voltage stresses of three capacitors), and its results showed that the secondary series capacitor was the most influential one. Tracking the secondary resonance frequency by measuring the secondary capacitance in real time to eliminate the error of the secondary capacitor was proposed then. The numerical method was used to find the optimal compensation parameters. Experiments were carried out and the results showed that the error tolerance was improved by 25.2% and the minimum power factor was increased from 0.78 to 0.89 when the designed ($k_{r\text{-}d}$, $k_{P\text{-}d}$, $k_{S\text{-}d}$) were changed from (1, 1, 1) to (1.040, 1.065, 1.100) and the secondary resonance frequency was tracked. The impacts of the proposed strategy on the constant primary coil current and voltage gain were also analyzed and tested, and the results proved that the excellent characteristics of the *LCC-S* compensation network remained unchanged, which validated the feasibility of the method proposed in this article.

References

[1] H. Feng, R. Tavakoli, O. C. Onar, and Z. Pantic, "Advances in high-power wireless charging systems: Overview and design considerations," *IEEE Trans. Transp. Electrific.*, vol. 6, no. 3, pp. 886–919, Sep. 2020.

[2] Z. Zhang, H. Pang, A. Georgiadis, and C. Cecati, "Wireless power transfer—An overview," *IEEE Trans. Ind. Electron.*, no. 2, pp. 1044–1058, Feb. 2019.

[3] J. Mai, Y. Wang, Y. Yao, M. Sun, and D. Xu, "High-misalignment-tolerant IPT systems with solenoid and double D pads," *IEEE Trans. Ind. Electron.*, vol. 69, no. 4, pp. 3527–3535, Apr. 2022.

[4] C. Cai, S. Wu, Z. Zhang, L. Jiang, and S. Yang, "Development of a fit-to-surface and lightweight magnetic coupler for autonomous underwater vehicle wireless charging systems," *IEEE Trans. Power Electron.*, vol. 36, no. 9, pp. 9927–9940, Sep. 2021.

[5] J.-Q. Zhu, Y.-L. Ban, R.-M. Xu, and C. C. Mi, "An NFC-CPT-combined coupler with series- none compensation for metal-cover smartphone applications," *IEEE J. Emerg. Sel. Topics Power Electron.*, vol. 9, no. 3, pp. 3758–3769, Jun. 2021.

[6] A. Hossain, P. Darvish, S. Mekhilef, K. S. Tey, and C. W. Tong, "A new coil structure of dual transmitters and dual receivers with integrated decoupling coils for increasing power transfer and misalignment tolerance of wireless EV charging system," *IEEE Trans. Ind. Electron.*, vol. 69, no. 8, pp. 7869–7878, Aug. 2022.

[7] *Film Capacitors—General Technical Information*. Tokyo, Japan: TDK, 2018. Accessed: Nov. 1, 2022. [Online]. Available: https://www.tdk-electronics.tdk.com/download/530754/480aeb04c789e4-5ef5bb9681513474ba/pdf-generaltechnicalinformation.pdf

[8] *Surface-mount ceramic multilayer capacitors*. Taipei, Taiwan: YAGEO, 2018. Accessed: May 1, 2022. [Online]. Available: https://www.jzic.com/goods/goods_pdf/495047.html

[9] M. H. El-Husseini, P. Venet, G. Rojat, and M. Fathallah, "Effect of the geometry on the aging of metalized polypropylene film capacitors," in *Proc. IEEE 32nd Annu. Power Electron. Specialists Conf.*, 2001, vol. 4, pp. 2061–2066.

[10] *Ceramic Capacitor Aging Made Simple*. Camarillo, CA, USA: Johanson Dielectrics Inc, 2021. Accessed: Nov. 1, 2022. [Online]. Available: https://www.johansondielectrics.com/downloads/ceramic-capacitor-aging-made-simple.pdf

[11] T. C. Feng, S. Duan, X. Zhang, H. Hu, and J. Niu, "A dual-side-detuned series–series compensated resonant converter for wide charging region in a wireless power transfer system," *IEEE Trans. Ind. Electron.*, vol. 65, no. 3, pp. 2177–2188, Mar. 2018.

[12] W. Zhang, S. Wong, C. K. Tse, and Q. Chen, "Design for efficiency optimization and voltage controllability of series–series compensated inductive power transfer systems," *IEEE Trans. Power Electron.*, vol. 29, no. 1, pp. 191–200, Jan. 2014.

[13] W. Zhang, S. Wong, C. K. Tse, and Q. Chen, "Load-independent duality of current and voltage outputs of a series-or parallel-compensated inductive power transfer converter with optimized efficiency," *IEEE J. Emerg. Sel. Topics Power Electron.*, vol. 3, no. 1, pp. 137–146, Mar. 2015.

[14] X. Zhang, F. Liu, and T. Mei, "Multifrequency phase-shifted control for multiphase multiload MCR WPT system to achieve targeted power distribution and high misalignment tolerance," *IEEE Trans. Power Electron.*, vol. 36, no. 1, pp. 991–1003, Jan. 2021.

[15] W. Liu, K. T. Chau, C. H. T. Lee, W. Han, X. Tian, and W. H. Lam, "Full-range soft-switching pulse frequency modulated wireless power transfer," *IEEE Trans. Power Electron.*, vol. 35, no. 6, pp. 6533–6547, Jun. 2020.

[16] H. Hu, T. Cai, S. Duan, X. Zhang, J. Niu, and H. Feng, "An optimal variable frequency phase shift control strategy for ZVS operation within wide power range in IPT systems," *IEEE Trans. Power Electron.*, vol. 35, no. 5, pp. 5517–5530, May 2020.

[17] Y. Liu, U. K. Madawala, R. Mai, and Z. He, "An optimal multivariable control strategy for inductive power transfer systems to improve efficiency," *IEEE Trans. Power Electron.*, vol. 35, no. 9, pp. 8998–9010, Sep. 2020.

[18] J. Tian and A. P. Hu, "A DC-voltage-controlled variable capacitor for stabilizing the ZVS frequency of a resonant converter for wireless power transfer," *IEEE Trans. Power Electron.*, vol. 32, no. 3, pp. 2312–2318, Mar. 2017.

[19] J. Zhang, J. Zhao, Y. Zhang, and F. Deng, "A wireless power transfer system with dual switch-controlled capacitors for efficiency optimization," *IEEE Trans. Power Electron.*, vol. 35, no. 6, pp. 6091–6101, Jun. 2020.

[20] Y. Wang, Z. Yang, and F. Lin, "Design and implementation of wireless power transfer systems with improved capacitor error tolerance," *IEEE Trans. Ind. Electron.*, vol. 69, no. 5, pp. 4707–4717, May 2022.

[21] A. Ramezani, S. Farhangi, H. Iman-Eini, B. Farhangi, R. Rahimi, and G. R. Moradi, "Optimized LCC-series compensated resonant network for stationary wireless EV chargers," *IEEE Trans. Ind. Electron.*, vol. 66, no. 4, pp. 2756–2765, Apr. 2019.

[22] Y. Geng, Z. Yang, and F. Lin, "Design and control for catenary charged light rail vehicle based on wireless power transfer and hybrid energy storage system," *IEEE Trans. Power Electron.*, vol. 35, no. 8, pp. 7894–7903, Aug. 2020.

[23] K. Song et al., "Constant current charging and maximum system efficiency tracking for wireless charging systems employing dual-side control," *IEEE Trans. Ind. Appl.*, vol. 56, no. 1, pp. 622–634, Jan./Feb. 2020.
[24] J. Mai, Y. Wang, Y. Yao, and D. Xu, "Analysis and design of high misalignment-tolerant compensation topologies with constant-current or constant-voltage output for IPT systems," *IEEE Trans. Power Electron.*, vol. 36, no. 3, pp. 2685–2695, Mar. 2021.
[25] A. Saltelli et al., "Variance based sensitivity analysis of model output: Design and estimator for the total sensitivity index," *Comput. Phys. Commun.*, vol. 181, pp. 259–270, Feb. 2010.
[26] W. Tian, "A review of sensitivity analysis methods in building energy analysis," *Renewable Sustain. Energy Rev.*, vol. 20, pp. 411–419, Apr. 2013.
[27] "Variance-based sensitivity analysis." Accessed: Nov. 1, 2022. [Online]. Available: https://en.wikipedia.org/wiki/Variance-based_sensitivity_analysis

Yi Wang (Graduate Student Member, IEEE) received the B.S. degree from the China University of Mining & Technology-Beijing, Beijing, China, in 2016, the M.S. degree from Beijing Jiaotong University, Beijing, in 2019, where he is currently working toward the Ph.D. degree with the School of Electrical Engineering, all in electrical engineering.

His research interests include power electronics and wireless power transfer technology.

Zhongping Yang (Member, IEEE) received the B.Eng. degree from the Tokyo University of Mercantile Marine, Tokyo, Japan, in 1997 and the M.Eng. and Ph.D. degrees from the University of Tokyo, Tokyo, Japan, in 1999 and 2002, respectively, all in electrical engineering.

He is currently a Professor with the School of Electrical Engineering, Beijing Jiaotong University, Beijing, China. His research interests include high-speed rail integration technology, traction and regenerative braking technology, and wireless power transfer of urban rail vehicles.

Prof. Yang received the Zhan Tianyou Award for Science and Technology in 2010, the Excellent Popular Science and Technology Book Award in 2011, and the Science and Technology Progress Award (second prize) of Ministry of Education in China in 2016.

Fei Lin (Member, IEEE) received the B.S. degree from Xi'an Jiaotong University, Xi'an, China, the M.S. degree from Shandong University, Jinan, China, and the Ph.D. degree from Tsinghua University, Beijing, China, in 1997, 2000, and 2004, respectively, all in electrical engineering.

He is currently a Professor with the School of Electrical Engineering, Beijing Jiaotong University. His research interests include traction converters and motor drives, energy management for railway systems, and digital control of power-electronic-based devices.

Jianning Dong (Senior Member, IEEE) received the B.S. and Ph.D. degrees in electrical engineering from Southeast University, Nanjing, China, in 2010 and 2015, respectively.

Since 2016, he has been an Assistant Professor with the DC System, Energy Conversion and Storage (DCE&S) Group, Delft University of Technology (TU Delft), Delft, The Netherlands. Before joining TU Delft, he was a Postdoctoral Researcher with McMaster Automotive Resource Centre, McMaster University, Hamilton, ON, Canada. His research interests include electromechanical energy conversion and contactless power transfer.

Pavol Bauer (Senior Member, IEEE) received the master's degree in electrical engineering from the Technical University of Kosice, Kosice, Slovakia, in 1985 and the Ph.D. degree in electrical engineering from the Delft University of Technology, Delft, The Netherlands, in 1995.

He is currently a Full Professor with the Department of Electrical Sustainable Energy, Delft University of Technology and the Head of DC Systems, Energy Conversion and Storage group. He received a title Prof. from the President of the Czech Republic at the Brno University of Technology in 2008 and the Delft University of Technology in 2016. He is also an Honorary Professor with Politehnica University Timisioira, Timisioira, Romania. From 2002 to 2003, he was working partially with KEMA (DNV GL, Arnhem) on different projects related to power electronics applications in power systems. He has authored over 95 journals and 350 conference papers in his field (with H factor Google scholar 39, Web of Science 29), he is an author or coauthor of eight books, holds nine international patents, and organized several tutorials at the international conferences. He has worked on many projects for industry concerning wind and wave energy, power electronic applications for power systems such as Smart-trafo; HVdc systems, projects for smart cities such as PV charging of electric vehicles, PV and storage integration, contactless charging; and he participated in several Leonardo da Vinci, H2020 and Electric Mobility Europe EU projects as Project Partner (ELINA, INETELE, E-Pragmatic, Micact, Trolly 2.0, OSCD) and Coordinator (PEMCWebLab.com-Edipe, SustEner, Eranet DCMICRO). He is the former Chairman of Benelux IEEE Joint Industry Applications Society, Power Electronics and Power Engineering Society chapter, Chairman of the Power Electronics and Motion Control (PEMC) council, Member of the Executive Committee of European Power Electronics Association (EPE), and also a Member of the International Steering Committee at numerous conferences.